TU Delft

Delft University of Technology

Course: Process Engineering & Thermodynamics

Course code: WB2543

Group: 5

Optimization on cost-effectiveness of PCM use in a photovoltaic cell

February 27, 2024

Authors:

Julian van den Bos (5141605)
Jelle Breed (5164435)
Naut Poelstra (4795342)
Liam Punselie (5123348)
Matthias Vink (5154499)
Lars Wassink (5116295)
Willem Wiersema (5168988)

Supervisor:

Dr. Lorenzo Botto

1 Introduction

Over the course of the past few decades, the demand for energy has been increasing rapidly. Most of the energy that is being generated still comes from methods that negatively impact the environment, such as fossil fuels and natural gases. More modern ways of generating energy include solar energy, most of which is generated by using an array of photo voltaic (further revered to as PV) cells. These cells absorb solar radiation and convert this partially into an electrical current which can be used as a power source. At the moment PV cells can only transform 15% to 20% of this absorbed radiation into usable energy, while the rest of the absorbed energy gets transformed into heat within the PV cell (Stropnik & Stritih, 2016). In combination with other external heat sources, such as ambient heat, the PV cells will warm up. This will negatively impact the performance of the cells. The loss of performance in turn leads to sub-optimal generation of energy.

A solution to this problem is presented by the use of a Phase Change Material (further revered to as PCM). When heated, a phase change material will, as the name suggests, change phase, while the temperature of the material stays constant. This property of certain materials could be exploited in order to keep a constant temperature in a device, which could prove useful in many different fields, such as the development of high-performance PVs that get exposed to high temperatures.

The main goal of this project is to model a simplified PV cell with a PCM. The model will be used to execute an optimization. In this report, we will discuss which PCM is best suited for the use of photo voltaic cells located in India. We will look into a suitable PCM that is the most profitable for PV cells by increasing its efficiency and thus optimizing its break-even point.

The report is structured as follows. Chapter 2 will briefly describe the background information of this problem and refers to previously done researches. A comprehensive overview of the literature review done can be found in chapter 3. The mathematical model of the PCM is discussed in chapter 4. The optimization of the PCM is preliminary discussed in chapter 5. The outcomes will be described in chapter 6. And a conclusion is given in chapter 7.

2 Background information

In this report, we will explore the benefits of a photovoltaic-phase change material system located in India, in an attempt to enhance the efficiency of the PV by choosing an eligible phase change material.

To understand the differences between phase change materials in photo voltaic cells, the following diagram from Li, Z. et al. (2019) gives insight in how different PCM materials affect the temperature ranges of the material. In this diagram, one can clearly see the difference between PCM1 and PCM2 for the PV-PCM system (the blue lines indicated in the graph below). While the temperature range of PCM2 remained relatively constant (between 31 – 39° Celsius), the temperature range of PCM1 was much wider (between 36 – 53° Celsius). This massive jump in PCM temperature is due to the fact that PCM1 already melted completely during the day (Li et al., 2019).

Therefore, it is very important to choose a PCM that does not melt completely during its day cycle, or, if it does, only for a very short duration in order to keep heat transfer to the PV to a minimum. By keeping the PCM in a specific temperature range, the PV device will maintain an optimum operating temperature, resulting in higher operating efficiency of the PV.

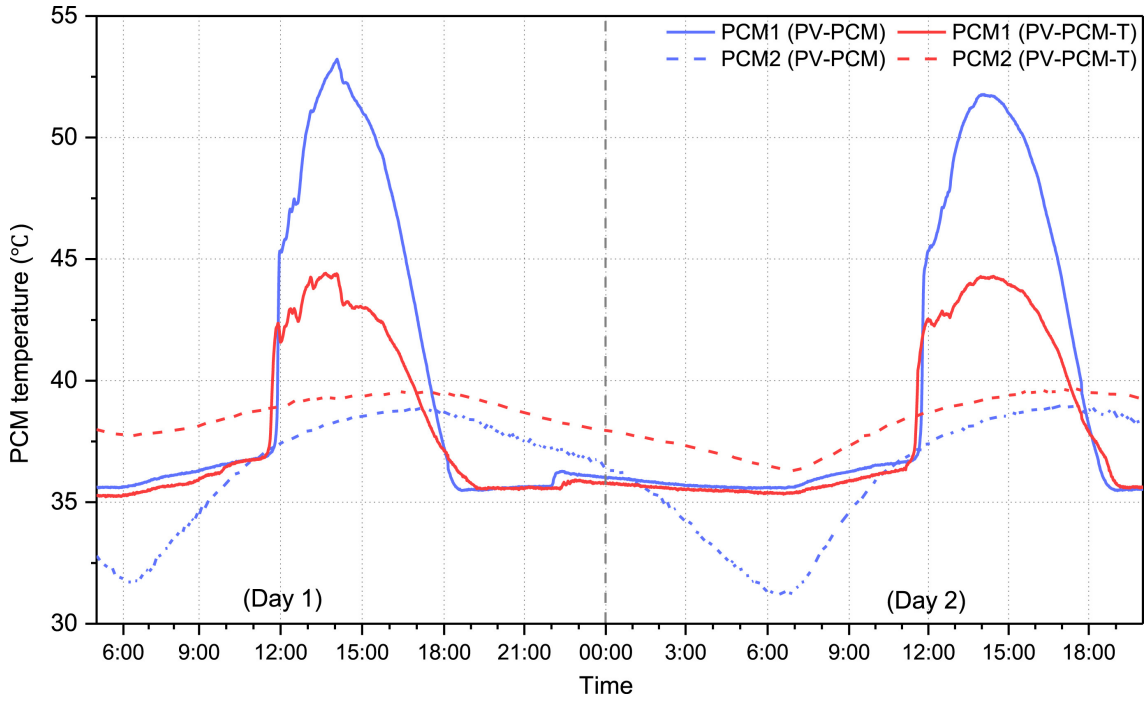

Figure 2.1: A graph showing the path of the temperature of 4 different PV/PCM units tested over a two day trial (Li et al., 2019).

3 Literature review

3.1 Heat transfer and storage

Heat transfer is used to store energy. It can be divided in three ways of transferring, namely heat conduction, heat convection and thermal radiation.

Conduction, thermal radiation and convection
To start, heat conduction is heat transfer through a wall for example.
Secondly, there is thermal radiation. All matter and space contains electromagnetic radiation. Heat transfer by radiation can be viewed either in terms of electromagnetic waves or in terms of photons (Mills A F, 2015).
Thirdly, there is heat convection. It means that the heat is transferred from a surface to a moving fluid or gas. For example a wall in air flow or water through a pipe.

Latent and sensible heat storage
Each of those examples can be divided into different ways that heat transfer takes place. There is latent heat storage and sensible heat storage. Latent heat storage: the total energy that is needed to change the material from one phase to another without changing its temperature. Sensible heat storage: the raise of the temperature of a solid or liquid by which heat is stored (Theodore L., 2011).

One of those storage methods is heat storage by thermal energy. An interesting one is the latent thermal heat storage, which uses the transition of the material. Latent heat storage stores the heat in the PCM (Wang et al., 2016).

3.2 Phase Change Material

Phase Change material simply means: a material that is transitioning from one phase to another. For example, ice melting or water condensing. While the material is changing phase, the temperature of this material will stay the same until all of the material has changed phase. Because of this a PCM can be used to keep an object or environment at a constant temperature while absorbing or emitting energy. PCMs are an attractive energy storage method for multiple reasons. A PCM can be used repeatedly, because it melts and solidifies over and over again. Also, different materials can be used as PCM. Because of this, there is a PCM for almost every temperature control situation. The most common and used ones are: SiO_2 and Al_2O_3 (Nomura et al., 2009).

3.3 Example of a PV/PCM unit

In figure 3.1 is a heavily simplified version of a PV/PCM unit illustrated. In reality a PV/PCM unit has more than four separate layers and exhibits more intricate heat flows and mechanics than depicted. However, since the goal of the example is to give an overview of the main parts and heat flows of such a unit, the simplification is favored.

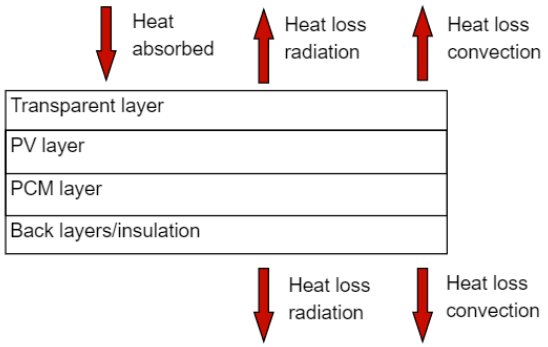

Figure 3.1: A simplified diagram of the main heat flows of a photo voltaic cell and PCM unit. Based on figures from Botto, 2020 and Smith et al., 2014.

The transparent layer is constructed out of a transparent material such as glass or a transparent polymer. This layer has to let through solar radiation for the PV cell while simultaneously protecting it from physical damage. The PV layer consists out of the photo voltaic cell which converts the captured solar light with a certain efficiency, which normally lies around 15 % to 20 %, into electricity (Stropnik & Stritih, 2016). The light that is not converted to electricity is dissipated as heat which heats up the entire PV/PCM unit. The heating of the unit will cause the efficiency to drop around 0.4 % to 0.65 % per degree, which is not desirable (Ma et al., 2015). This is were the PCM layer comes into play, the function of this layer is to absorb the excess heat of the PV/PCM unit to keep the temperature stable around the optimal operating temperature of the PV cell. If this is the case then there will be minimal efficiency losses of electricity generation. The last layer is constructed out of multiple back layers of material with a high conductivity because this increases the performance of the unit (Hasan et al., 2010; Smith et al., 2014).

The figure 3.1 also displays the main external heat flows (heat flows that interact with the PCM/PV unit and the surroundings), of which there is one that flows inwards. The inward bound flow is caused by radiation of the sun and by heat absorbed in the air depending on the temperature of the PV/PCM and the air itself. The other four heat flows, which transfer heat out of the unit, are the work of convection between the unit and the ambient air and radiation from the unit. In this optimization research the heat loss through the

sides of the unit is neglected. In chapter 6 there will be a more detailed explanation of the heat flows that interact with the PCM/PV unit.

3.4 Photovoltaic cells

Photovoltaic cells, also called solar cells, convert energy of the sun into electricity. The earths atmosphere breaks the light of the sun and absorption takes place. This reduces the intensity and the distribution of the wavelength of the sunlight that reaches the earths surface (Wenham, 2011). PV is one of the cheapest forms of electrical energy (Contributors to Wikimedia projects, 2020).

Efficiency of a photovoltaic cell
In photovoltaic cells only a small percentage of the heat is transformed into electricity. The rest of the heat is heating up the solar cell which lowers the producing of electricity. So, with a higher temperature, the more heat is released, the lower the electricity income of the PV. The nations with a higher light density have a more effective solar cell (Wu et al., 2019).

4 General description of the mathematical model

4.1 Heat transfer

Conservation of energy states that $\Delta U = Q - W$. A lot of the time work effects are negligible when analysing heat transfer (Mills A F, 2015). So we can also write the heat balance as $\Delta U = \dot{Q} + \dot{Q}v$ which reads as: *change internal energy of the system = net heat transferred into the system + heat generated within the system*

For closed systems with a fixed mass of a solid, the heat balance follows: $\Delta U = \rho V c \frac{dT}{dt} = \dot{Q} + \dot{Q}v$. Since $\Delta U = \rho V du$ with du being the specific internal energy. If the solid is then also incompressible then $du = c_v dT$ and c_v is the constant-volume specific heat.

As found in (Mills A F, 2015). For an open system you can use the **steady-flow energy equation**: $\dot{m}\Delta(h + \frac{V^2}{2} + gz) = \dot{Q} + \dot{W}$.

As mentioned earlier in section 3.1.1 there are 3 types of heat transfer: heat conduction, convection or thermal radiation. Each have their own mathematical formulae and will be mentioned and explained in this next section.

4.1.1 Heat conduction

An other essential equation is **Fourier's law of heat conduction**: $q = -k\frac{dT}{dx}$ where k is the **thermal conductivity** of the substance in W/m K (Mills A F, 2015).
And q is called the **heat flux** which is also defined as $q = \frac{\dot{Q}}{A}$ where A is the surface through which heat transfer takes place. Combine these 2 expressions and you can deduce the following equation $\dot{Q} = \frac{T_1 - T_2}{R}$ where $R = \frac{L}{kA}$ and is the **thermal resistance** (Mills A F, 2015).

4.1.2 Heat convection

Heat flux caused by convection is defined with *Newton's law of cooling* and is in the case of a PCM exposed in air: $q_{conv} = -h_{air}\Delta T$ where h_{air} is the **convective heat transfer coefficient**. This coefficient depends on the used material and it's properties.

4.1.3 Thermal radiation

Thermal radiation can be subdivided into long wavelength radiation and short wavelength radiation. The difference between the two is in the case of a PCM with a PV cell very clear. The solar radiation of sunlight upon the PCM, also called solar irradiation, is in the short wavelength region of the spectrum. While the absorption or emissivity of any surface is at much longer wavelengths. Thus a solar surface absorptive quality also depend on it's emissivity ε (Theodore L., 2011). Heat flux due to long wavelength radiation is: $q_{longwave} = \sigma(\varepsilon_{air} T_{air}^4 - \varepsilon T^4)$

When the PCM is exposed to the air, the relationship of Swinbank is more suitable for: $T_{air} = T_{sky} = 0.0552 T_{air}^{1.5}$ (Smith et al., 2014)
$q_{shortwave} = (1 - \eta)\alpha I$ with I being the sun irradiation on the PCM, α is the absorptive ability of the PV cell and η is the efficiency of the PV cell: $\eta = max(0, \eta_{ref}[1 - \beta(T - T_ref))]$ with η_{ref} being the efficiency of the PV at T_{ref} and β being the thermal expansion coefficient which depends on the type of fluid used in convection. For a perfect gas: $\beta = \frac{1}{T}$.

4.2 Boundary conditions

Because the liquid and the solid states of the PCM both have a linear temperature profile, the temperature profile can easily be described by a set of linear equations. For this, Fourier's law can be used: $q = -k(\frac{\partial T}{\partial x})$ where q is the heat flux and k is the thermal conductivity of the material. This equation is then rewritten to describe the situation at the begin and the end of the PCM. In other words, for $x = 0$ and $x = L$. For $x = 0$ the formula adapts to: $q_0 = -k_l(\frac{T_{melting} - T_0}{x_{melting}})$ and for $x = L$ the formula adapts to: $q_L = -k_s(\frac{T_L - T_{melting}}{L - x_{melting}})$

For these formulas the position of the melting front has to be known. This can be solved by making an energy balance of the fluxes in the melting front: $\rho h_{sl} v_{melting} = -k_l(\frac{T_{melting} - T_0}{x_{melting}}) + k_s(\frac{T_L - T_{melting}}{L - x_{melting}})$

As found in Mills A F, 2015. When this is solved for $v_{melting}$ the position of $x_{melting}$ can be calculated by numerical integration.

5 Preliminary discussion of the model

The goal of our project is to find a PCM that it is the most profitable for our PV cell and thus returns it's investments the fastest. The PCM also needs to stay close to the ideal operating temperature of the PV. The variables that we choose to optimize of a PCM are: melting temperature, latent heat and the cost price per gram.

5.1 Properties PCM

Considerations about the variables
Looking to the cost price the different PCMs have, there are a few promising PCMs. All these different materials have properties like density, latent heat, enthalpy and so on. These different variables can be used to calculate the efficiency of the specific material. After a little research it came out that it is very hard to find a decent amount of variables to calculate with. Therefore, a choice has been made which variables will be used to calculate the efficiency. That means the calculation does not take all the variables in account. The other variables are also recommended, but for this optimization is chosen to use the mean value of PCM properties. These properties (Smith et al., 2014) are visible in the report in table 6.1. The only properties that are known for each PCM are the latent heat, the melting temperature and the cost price per gram (Chemicalbook, 2021). In the calculation we will use these mentioned variables.

5.2 Variables

There are multiple variables that have an impact on the performance of the PCM. The variables that are not constant through out the calculation will be briefly discussed below.

Cost price per gram
The cost price per gram of each PCM is important for the calculation of the reinvestment time of the PCM. If two PCMs have the same parameters but one of the two has a higher cost price per gram material, it will take that PCM longer to reach its break-even point. On the other hand, the more expensive PCMs tend to have a higher latent heat and will therefore be more efficient since they can absorb more energy.

Latent heat
For the PCM that is used, the latent heat is the amount of heat that is absorbed when the PCM goes from solid to a liquid phase. A higher latent heat means the material can absorb more heat while staying at the melting temperature. If you compare two PCMs with the same heat flux and thermal conductivity, but with a different latent heat, the one with a higher latent heat will absorb more energy. And it will also absorb energy over a longer period of time.

Melting temperature
The melting temperature is the temperature at which the PCM changes from a solid to a liquid phase. This is the temperature of the melting front in the melting process. This influences the temperature of the PV-cell and therefore the efficiency of the PV-cell.

5.3 Aspects not accounted for within the numerical model

Since the numerical model of the PCM is only a model of reality, there are expected deviations in performance when tested in real life. These deviations are the product of assumptions, simplifications and idealizations made in the code to make the project feasible to construct within a certain time frame. Additionally the code is adopted to counter over-complication and limit processing time. Because of this there are certain aspects of real life which are not accounted for in the numerical model, which will be discussed below.

Variability of the weather
Because the point of interest was to compare the performance of different PCMs relative to each other the variability of the weather is not considered relevant, as long as all PCMs are simulated with the same weather conditions. Therefor the PCMs are studied along a clear, windless 8-hour day with a constant solar irradiance of 700 W/m^2. This is determined by the fact that India is our PV location and using for this data Solargis, 2020 has been used.

PCM pricing and costs
Another aspect that had to be simplified is the cost of the PCMs, in the model a constant PCM price is assumed for each PCM. But due to a market that is continuously evolving there isn't such a thing as a constant price for a PCM. For the salt hydrates and non-paraffins price ranges wildly varied but were readily available in contrast to the paraffins prices which were hardly obtainable. For this reason the choice was made to model with a constant price for all the parrafin PCMs, this price was obtained from Aroatech, 2021. Regarding the salt hydrates and non-paraffins, the main reason for the disparity was the purity of the material. Since the relation between purity and the PCM's cost and performance were outside the scope of this project it was decided that the cheapest material price per gram would be taken as the constant PCM price for that particular PCM. These prices were collected from Chemicalbook, 2021 and evaluated in Excel, ChemicalBook was chosen because the site displays offers from multiple manufacturers and bulk orders to accurately simulate industry prices. Other costs such as manufacturing costs of a PCM unit and maintenance costs are left out of the model on the grounds that these costs are assumed to be relatively the same for each PCM and for the sake of over-complication of the model.

Sustainability and Toxicity
Although sustainability and toxicity play a significant role in the current environment, they were not considered in the selection of the different PCM materials. Considering these aspects would greatly complicate

the numerical model and intensify the research, which was not possible during this project.

Value of power
In the numerical model there is an assumption that all the power generated will be sold for a constant price of 0.49 $\$/kWh$ (Baker & Kalowenkamo, 2009). In reality these prices are fluid and rely on demand and supply, so again are the forces of the free market neglected to simplify the model. Another idealization is that in reality power cannot always be sold if there is a surplus of power. However, these problems are not relevant for the research question of the project and thus left out of the model.

Heat loss of the PV/PCM unit
Though heat loss from the PV/PCM from the top and bottom sides is accounted for in the model, heat loss from the sides of the units is neglected. Assuming the heat loss from the sides is negligible relative to the heat loss from the top and bottom (Smith et al., 2014).

Heat absorption after liquefying PCM
In the numerical model the simulation of the PV/PCM unit stops after the PCM is fully melted, naturally the unit will continue to heat. The assumption made here is that the unit will warm along a linear path after the PCM is fully liquefied (Botto, 2020). Since this trajectory is the same for each PCM and only dependent on the temperature at the end of the melting of the PCM, this region is not of the interest of the project. On the grounds that the differences in performance of the PCMs are made in the region where the PCMs are still melting. This is namely the reason that effects the temperature of the PCM at the end of the melting region.

Cooling of PV/PCM during the night
At last it is assumed that the PV/PCM units completely cool down to the local air temperature by the end of the night, which in this model is defined at 303 K (Solargis, 2020). In other words the units will always have a starting temperature of 303 K without regard to nightly conditions. In reality this is not necessarily true and is dependent on the local air temperatures during the night, the temperature of the PV/PCM unit at the end of the day and weather conditions such as rain or wind. As said earlier variable weather conditions are not considered for the sake of relevancy and over complication, which also applies during the night.

6 Results of the model

6.1 Parameters

Let's discuss the exact values for the parameters in the code. In table 6.1 the average values of a PCM are shown (Smith et al., 2014) along with the other constant parameters. As discussed in chapter 5 there are some assumptions made in our model. These assumptions result in the following values for certain parameters: a) The area of PCM is set to a fixed 1 square meter. This is just an arbitrary constant. The same goes for the thickness of PCM. These parameters are not relevant in this optimization, as long as they remain the same for each PCM in order to effectively compare them to each other. b) The time (t) for this PCM process is 8 hours which simulates 1 whole day. In our model this is converted to seconds, so 28800 seconds in total means 1 day has ended. c) The irradiance and air temperature are determined by the location of the PV cell, which is in this case India. The main interest of the optimization is when the air temperature is high. That is the moment that the PV cell loses most efficiency. The use of a PCM would be most beneficial. This is why the temperature of air is set to 303 K. This is the higher range of the average summer temperature in India(Solargis, 2020) which is our chosen PV/PCM unit location. Parameters T_{ref}, η_{ref} and β are simply taken from (Smith et al., 2014).

Constant Parameters			
Type	symbol	value	units
PCM density	ρ	800	kg/m^3
PCM liquid thermal conductivity	k$_l$	0.15	W/(m K)
PCM solid thermal conductivity	k$_s$	0.24	W/(m K)
Heat transfer coefficient of air	h$_{air}$	8.9	W/(m^2K)
Stefan-Boltzmann coefficient	σ	5.7*10^{-8}	W/(m$^2K^4$)
Emissivity of air	ε	0.95	-
Emissivity of PCM	ε	0.90	-
Coefficient of thermal expansion	β	0.0045	K^{-1}
Area of PCM	A	1	m^2
Thickness of PCM	L	0.01	m
Temperature air	T$_{air}$	303	K
Irradiance	I	700	W/m^2
Absorptance of PV cell	α	0.9	-
Reference Temperature	T$_{ref}$	298	K
Efficiency at reference Temperature	η_{ref}	0.156	-
Specific heat capacity PCM solid	c$_p$	2900	J/(kg K)
Time	t	0-28800	s
Mass	m	$\rho * A * L$	kg
Time step	dt	1	-

Table 6.1: The values of all constant parameters

6.2 In depth explanation of code simulation

The PCM heating process is simulated in the code.This can be described in the following way, also depicted in figure 6.1

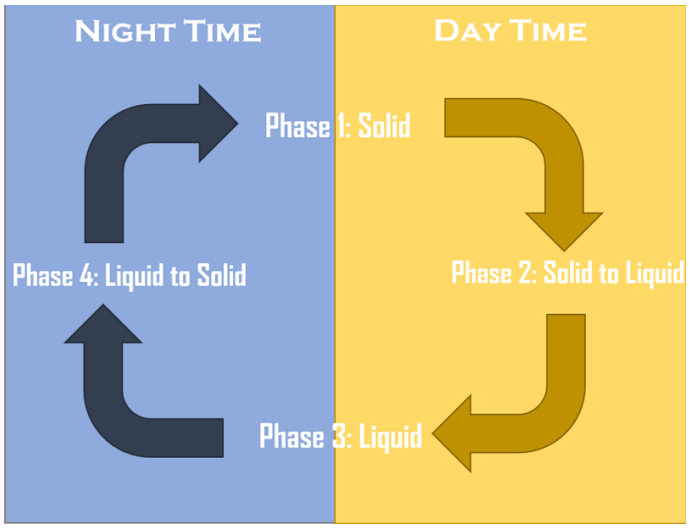

Figure 6.1: The Day-Night cycle of the PCM

Phase 1: Solid
The PCM has the same temperature as it's surroundings, the air temperature. The PCM thickness is very small and to simplify our model an assumption is made: the PCM will heat as if it is a homogeneous solid in this phase. This means that there is a linear temperature profile. As soon as the temperature of the PCM

reaches its melting temperature phase 1 stops. The next assumption is that the top part of the PCM will be the warmest. So the temperature at the top of the PCM will be equal to the melting temperature at the end of phase 1. To make the transition to phase 2 possible, the location of the melting front is defined at the end of phase 1. This is set at a very small number from the top (x=0.00001 m)

Phase 2: Solid to Liquid
In this phase there is a melting front in the PCM with a certain speed and location (x). The melting front is the place between the solid and liquid part of the PCM and its temperature is equal to melting temperature. This front moves through the PCM from x=0 to x=L with L being the PCM thickness. Phase 2 starts as soon as there is a melting front and when the top temperature of the PCM equals the melting temperature. The temperature profile is in this phase determined by calculating the temperature at the top(x=0) and bottom(x=L) of the PCM. When the temperature at the bottom equals the melting temperature phase 2 stops.

Phase 3: Liquid
This phase is irrelevant for our optimization. In phase 3 the whole PCM is melted and can still heat up as a whole liquid. But since the main interest of this model is in prolonging phase 2, phase 3 is not included in the code.

Phase 4: Liquid to Solid
In reality the PCM will go from a totally liquid state back to a completely solid phase. For simplification the assumption is made that the PCM will be fully solid after every night. So that the next day the PCM starts as a solid.

Calculations
The speed of the melting front is numerically calculated with the rewritten formulae from chapter 4: $v_{melting}[n] = (-k_l * (((T_{melting} - T0[n])/(x[n])) + k_s * ((T_l[n] - T_{melting})/(L - x[n])))/(\rho * h_{sl}))$ with h_{sl} being the latent heat. The total heating of the PCM can be written in 3 equations (Smith et al., 2014):

$$\text{Convection: } q_{conv} = h_{air} * (T_{air} - T_0) \tag{6.1}$$

$$\text{Long wave radiation: } q_{lw} = \sigma * (e_{air} * (T_{sky}^4) - (e_{pcm} * (T0^4)) \tag{6.2}$$

$$\text{Short wave radiation: } q_{sw} = (1 - f_{eta}(T_0)) * \alpha * I \tag{6.3}$$

The total heat flux going in the PCM is: $q_0 = q_{conv} + q_{lw} + q_{sw}$. The heat flux out of the PCM at the bottom has 2 parts: Convection and long wave radiation. Thus the total flux of the PCM at the bottom equals: $q_L = q_{conv} + q_{lw}$. The efficiency of the PCM is calculated with the function f_{eta} which is based on the formulae form chapter 4 Thermal radiation.

The temperature profile in phase 1 is $T0[n] = T0[0] + ((q_0[n] - q_L[n])/(c_p * m)) * t[n]$. Which is a numerical calculation where the initial value of the temperature is added to the calculation of heat flux in minus heat flux out multiplied by the time. This is done during the time for 1 day indicated with t.

The temperature at x=0 in phase 2 is $T0[n] = ((q0[n] * x[n])/k_l) + T_{melting}$. This is also a numerical calculation done in the same way as in phase 1. The only difference is that there are 2 calculations: one for T_0 at x=0 and one for T_L at x=L. The second calculation is $T_l[n] = ((qL[n] * (L - x[n]))/k_s) + T_{melting}$ for the temperature at the bottom. The location of the melting front(x) is numerical calculated with $x[n+1] = x[n] + v_{melting}[n] * dt$

6.3 Break-even time

The optimization is as follows: there will be a function for the total cost of the PCM, including the PV-cell. This will be determined by the price of the PCM material and the amount of material needed. A list of already existing PCMs will be ran through our calculations to find the most effective ones to increase the efficiency of the PV. Each of these PCMs have set thermal properties, but as discussed in chapter 5 the average properties of a PCM will be used, these are listed in table 6.1 . Then the duration till the break-even point will be computed. So, in the end the most profitable PCM for a PV cell which returns it's investments

the fastest can be found. For the calculation and simulation of the optimization a code has been made in *Python* of the PV cell with PCM, previously explained in this section.

Explanation return on investment time code
To calculate the time it takes for a PV cell to reach its break-even point the following equations are used: $Cost_{total} = Cost_{PV} + Cost_{PCM}$. First, the total cost of the PV cell, with the PCM layer included, is calculated. The cost of the PV cell is considered to be a constant \$140 (Baker & Kalowenkamo, 2009). The cost of the PCM is different for each PCM. The cost of the PCM is calculated by the following formula: $Cost_{PCM} = A * L * y * \rho$ with y being the cost price of the PCM. Then the average efficiency of the PV cell with the PCM is calculated to find the power and profit that is generated by the PV cell each day. This is done by calculating a mean value for the function f_{eta}. The energy saved or that is extra converted by the PV due to the PCM is also calculated. We have called this the Power of the PCM: $Power = I * \eta_{avg}$ and $Profit = Power * Price_{electricity}$ When the profit per day is known, the amount of days it takes a PV cell with a certain PCM to reach its break-even point can be calculated: $t_{break-even} = Cost_{total}/Profit$.

6.4 Results

6.4.1 Paraffins

Below, the results of 4 paraffins functioning as phase change material will be displayed. The temperature at the top and the bottom, and the speed of the melting front figure are shown as a function of time.

Paraffins as PCM					
Paraffin	$T_{melting}$ (°C)	Latent heat (KJ/kg)	Material costs (\$/g)	Break-even point (days)	Extra energy converted (J)
C_{21}	40.2	200	0.165	122	24
C_{22}	44	249	0,165	87	34,36
C_{24}	50,6	255	0,165	63	47
C_{26}	56,3	256	0,165	45	66,21

Table 6.2: A table containing 4 paraffins with the variables used in the numerical model ($T_{melting}$, latent heat and material costs) and the results found when running the PCMs through the model. Denomination is on the number of carbon atoms e.g. C_{21} means that the parraffin molecule contains 21 carbon atoms.

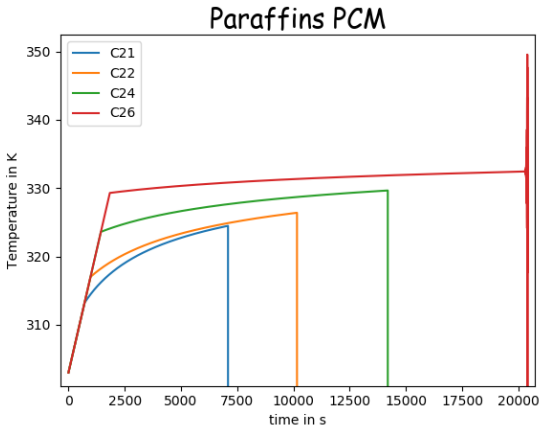

(a) The temperature at the top of the PCM layer of the 4 different paraffins plotted against time.

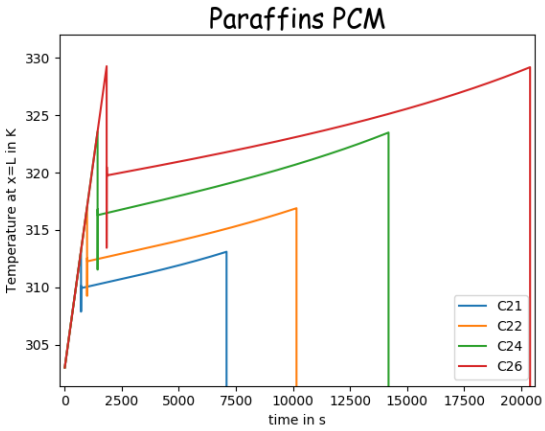

(b) The temperature at the bottom of the PCM layer of the 4 different parrafin's plotted against time.

Figure 6.2

In figure 6.2a The temperature increases linear at first until the melting temperature is reached, after that the PCM starts to melt and the temperature function changes to a hyperbolic function, which is less steep then the linear part. The spike of paraffin C_{26} at the end of the graph can be explained by the fact that the temperature is numerically calculated. This results in the PCM reaching its limit value as the melting front position X approaches L and thus the code becomes unstable. To prevent this from happening a correction error has been used so the code will stop just before x=L. For the C26 Paraffin this correction is too small.

In figure 6.2b there is a drop in temperature around, depending on the PCM, t = 1500 seconds which has to do with an assumption. Before the melting it is assumed that the temperature of the PCM is uniform since the layer is relatively thin. When the temperature reaches $T_{melting}$ the top of the it is assumed to have the highest temperature. Which results in the temperature at the bottom being lower and therefore connects the second part of the graph also lower. At the end of both graphs the temperatures drops to 0 since the graphs are not defined in the liquid phase. Therefore it can be ignored.

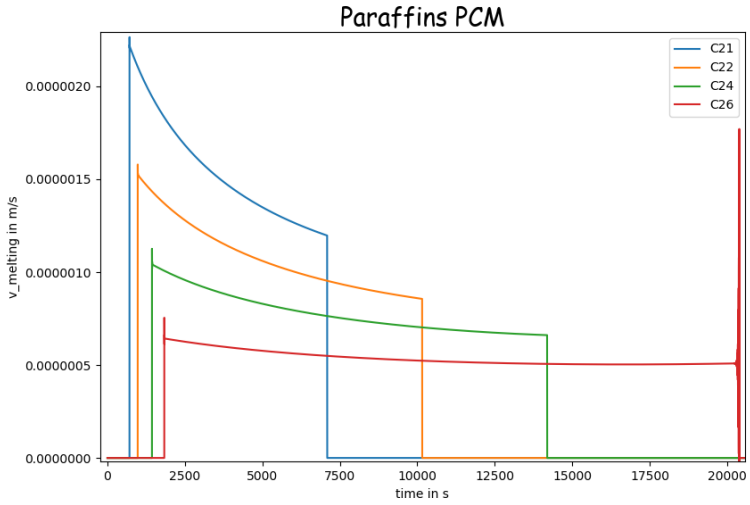

Figure 6.3: The speed of the melting front of the 4 paraffins as PCMs plotted against time.

Figure 6.3 shows the speed of the melting front. The graphs start when the melting temperature is reached and end when the whole PCM has melted. Due to the code there are fluctuations in the graphs, when the melting has started, the code gives the melting front a very small value. It is necessary in the formula for the velocity of the melting front, to divide by the position of the melting front. This approaches a division by zero and this produces these fluctuations. The mathematical area under the graphs are all the same, since that is equal to the thickness(L) of the PCM. It is beneficial that the melting speed is as low as possible so the PCM stays around the desired temperature for the longest period. When the PCM has a high melting temperature it takes longer before it starts to melt, however with these paraffins the higher the melting temperature, the higher the latent heat, as shown in table 6.2. Therefore the melting process duration also is the longest. This is the case for the paraffin C_{26} which is the best PCM of the paraffins.

In conclusion of the paraffins the one with 26 carbon atoms is the most efficient one. They were all equally expensive as shown in table 6.2. Therefore it is also the best performing paraffin.

6.4.2 Non-Paraffins

Non-Paraffins as PCM					
Non-Paraffin	$T_{melting}$ (°C)	Latent heat (KJ/kg)	Material costs ($/g)	Break-even point (days)	Extra energy converted (J)
Caprylone	40	259	12,6	6761	30,46
4-Heptadacanone	41	197	31,289	20653	24,75
9-Heptadecanone	41	213	9,6	5918	26,5
Cyanamide	44	209	0,105	68	29,4

Table 6.3

Here the results of 4 Non-paraffin materials is displayed. The temperature on top and at the bottom, and the speed of the melting front are shown as a function of time.

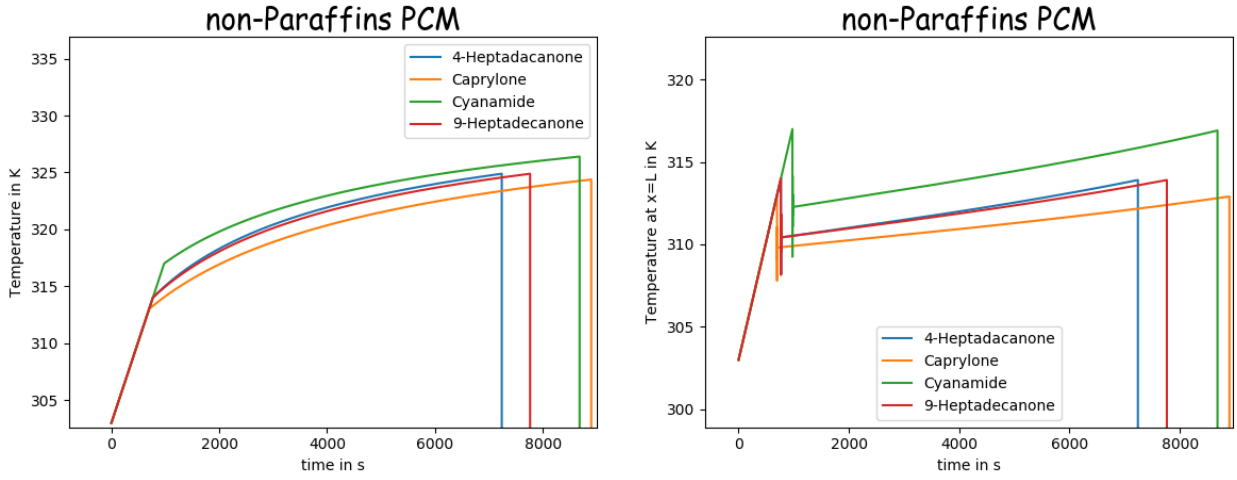

(a) The temperature at the top of the PCM layer of the 4 different non-paraffin's plotted against time.

(b) The temperature at the bottom of the PCM layer of the 4 different non-paraffin's plotted against time.

Figure 6.4

In figure 6.4a the temperature increases linear until the melting temperature is reached. Then it changes to a hyperbolic function and the PCM starts melting. Around t = 800 seconds the curve of figure is not

smooth. This is because of the way our code works. When the melting temperature is reached a different part of the code is activated creating a discontinuity. Because the PCM is melting the temperature increases slower from t = 900 onward. At the end of the graph the lines drop to 0, this can be ignored because at that point the entire PCM is in liquid phase and the model is not defined beyond that point.

In figure 6.4b, the temperature at the bottom at first increases linearly with time. Around t = 900 seconds there is a jump in the function, this occurs because the temperature of the PV-cell is assumed to be uniform until the melting temperature is reached. When the melting temperature is reached at the top of the PCM, the temperature at the bottom of the PCM drops to its intended value. After this, the temperature rises until the melting temperature is reached. At this point, the entire PCM is liquid and the code stops.

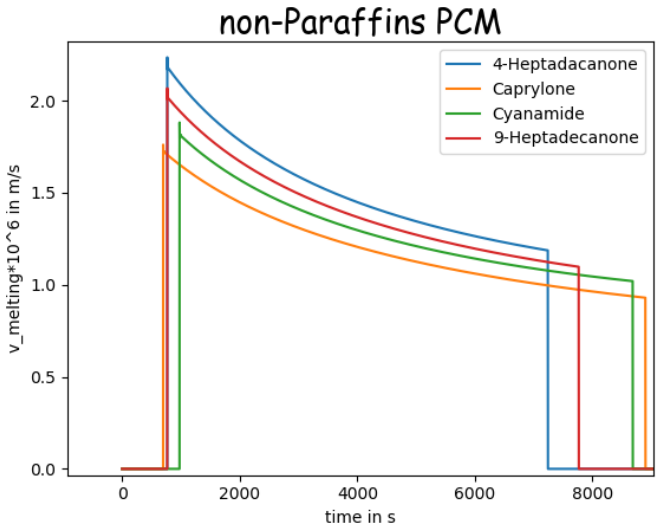

Figure 6.5: The speed of the melting front of the 4 non-paraffin's as PCMs plotted against time.

This graph starts when the melting temperature for the top of the PCM is reached, around t = 900. The speed of the melting front is shown in figure 6.5. When all of the PCM has melted the speed will drop to 0. A low melting speed is desired, because this means the PCM will absorb more energy. When the entire PCM has melted the speed of the melting front is zero as seen in the graph.

From the non-paraffin PCM materials, 'Caprylone' shows the best results in terms of heat absorption. This was expected because it has the highest latent heat, it is also a relatively expensive material, as shown in table 6.3. Cyanamide is relatively cheap and still shows good results, this would be a better option in terms of cost effectiveness.

6.4.3 Fatty Acids

Fatty acids as PCM					
Fatty acid	$T_{melting}$ (°C)	Latent heat (KJ/kg)	Material costs ($/g)	Break-even point (days)	Extra energy converted (J)
Elaidic Acid	47	218	63,2	29825	35
Lauric Acid	49	178	0,294	160	32,1
Tristearin	56	191	0,36	123	49,95
Palmitic Acid	55	163	0,683	281	40,76

Table 6.4: A table containing 4 fatty acids with the variables used in the numerical model ($T_{melting}$, latent heat and material costs) and the results found when running the PCMs through the model.

Here the results of 4 fatty acids functioning as PCMs will be displayed. The temperature on the top and the bottom, the speed and position of the melting front are shown as a function of time.

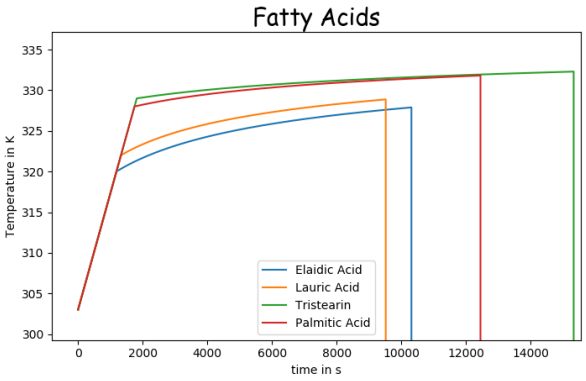

(a) The temperature at the top of the PCM layer of the 4 different fatty acids plotted against time.

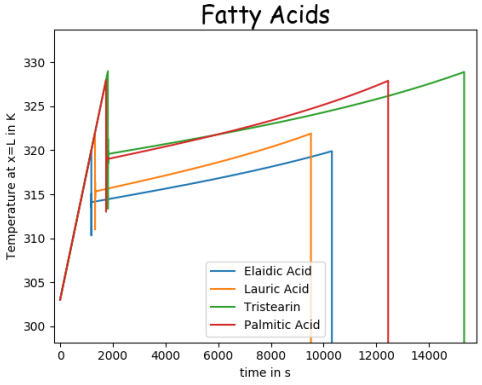

(b) The temperature at the bottom of the PCM layer of the 4 different fatty acids plotted against time.

Figure 6.6

Graph figure 6.6a consists of two line segments. The function starts linearly and, as the temperature approaches the melting temperature, the function will change to a different function that looks to be hyperbolic. There is a sudden change in the graphs, which occurs between t = 1200 and t = 1800 depending on the material of the PCM. This occurs spontaneously as opposed to a smooth transition in the curve. Since this is not within the scope of our optimization research, we acknowledge this anomaly but won't investigate it any further.

What we see in this graph is that for the four fatty acids that we modeled, tristearin takes the longest time before melting completely (in just under 15000 seconds, equally to about 4 hours). This is a interesting result as tristearin is the cheapest of the four fatty acids. This long melting time also makes it the best PCM material in it's class for use in a PV cell assembly for heat absorption.

Figure 6.6b shows the relation between the temperature at the bottom of the PCM with respect to time. We can clearly distinguish two segments of the graph. Part one is a linear part which occurs between t = 0 and t = 2000 depending on the material for the PCM. This linear part is the temperature while the PCM is still solid. Part two is a parabolic part which occurs when the melting front passes through the PCM. During the transition between solid to solid-liquid phase, we see a huge jump in the graphs.This is due to the same reason as explained for paraffins and non-paraffins. Again, because we go from heating as a homogeneous solid to heating at the top and bottom of the PCM, this explaines the discontinuity.

When the melting front gets further away from x = 0, the graph will move consistently until the melting front reaches x = L, which is when the code ultimately breaks and this is indicated by the large jump at the end of all the plotted functions.

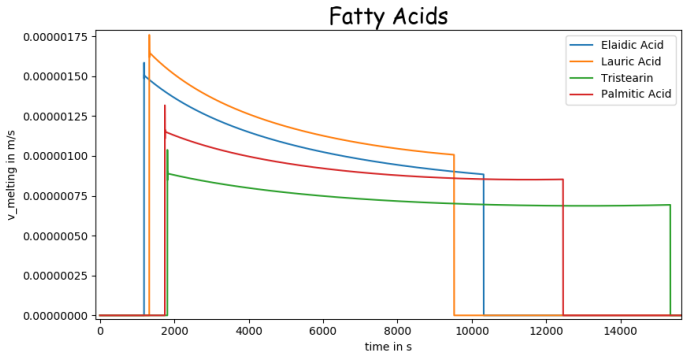

Figure 6.7: The velocity of the melting front of the 4 fatty acids as PCMs plotted against time.

In this plot, figure 6.7, we can see the relation between the velocity of the melting front with respect to time. All functions initially start at zero since the melting front doesn't exist when T0 is less than the melting temperature for the respective material. As soon as T0 is equal or greater than the melting temperature, the melting front will begin to move. The velocity of the melting front will stay greater than zero until the boundary condition of x = L is met, which means that the melting front has passed through the entire PCM. At this point, the function will break and the velocity of the melting front will be set to zero.

When the functions transition from velocity = 0 to velocity = N where N is the highest value of $v_{melting}$ of the PCM, we can see a big jump. And when zoomed in we can see an oscillating function which dampens out after a short time. This happens because when the melting front is at a location very close to the top of the PCM, it will tend to infinity and blow up the code. In order to mitigate this, we set x to a value very close to 0 manually in order to prevent this from happening, but in doing so it will still cause a short time where the function 'spikes'. Therefore, we will ignore the interval where this occurs since it is not relevant for this study.

It is interesting to note that the velocity of the melting front for tristearin remains the lowest out of all PCMs. It also makes sense, since the lower the velocity of the melting front is, the 'longer' it takes for the melting front to reach the other end of the PCM. It is therefore beneficial to have a PCM with a low velocity of the melting front since it allows the PCM to stay in the solid-liquid phase for a longer period of time and the most heat absorption takes place.

6.4.4 Salt hydrates

Salt hydrates as PCM					
Salt hydrate	$T_{melting}$ (°C)	Latent heat (KJ/kg)	Material costs ($/g)	Break-even point (days)	Extra energy converted (J)
$CoSO_4 \cdot 7\,H_2O$	40,7	170	0,348	278	21,47
$K_2HPO_4 \cdot 7\,H_2O$	45	145	0,16	129	22,4
$Na_2S_2O_3 \cdot 5\,H_2O$	48,5	210	0,03	22	35,82
$FeCl_3 \cdot 2\,H_2O$	56	90	0,014	19	26,88

Table 6.5: A table containing 4 salt hydrates with the variables used in the numerical model ($T_{melting}$, latent heat and material costs) and the results found when running the PCMs through the model.

Here the results of 4 salt hydrates will be displayed. The temperature on top, at the bottom, and the speed of the melting front are shown as a function of time.

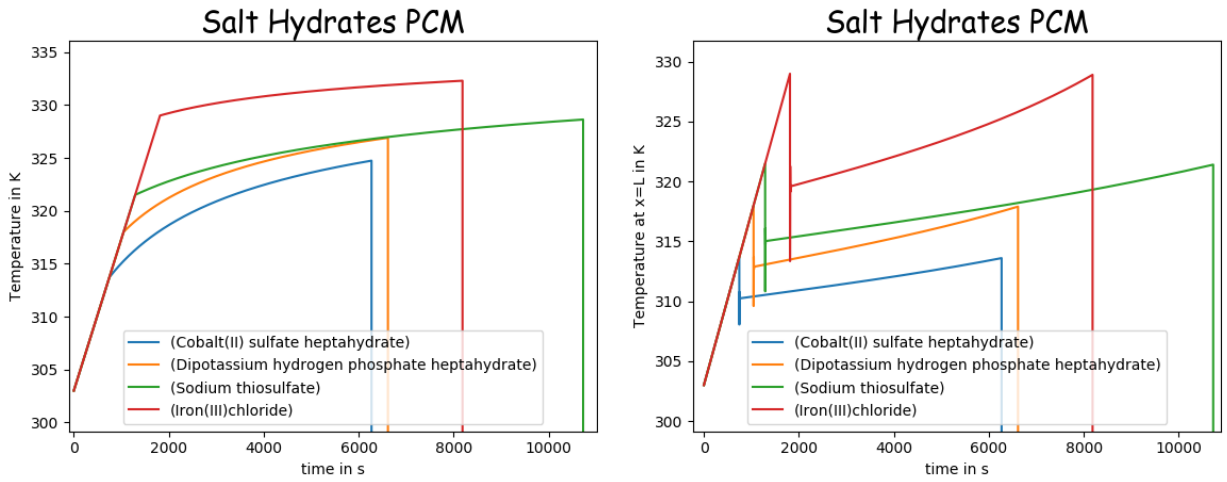

(a) The temperature at the top of the PCM layer of the 4 different salt hydrates plotted against time.

(b) The temperature at the bottom of the PCM layer of the 4 different salt hydrates plotted against time.

Figure 6.8

Figure 6.8a shows the temperature at the top of the PCM for 4 salt hydrates. The temperature increases linear at first and later changes to a melting front when the melting temperature has been reached. This causes a discontinuity that can be ignored because its not in the scope of the optimization. The graph ends when all the PCM has melted, the temperature drops to zero at that point because the code is not defined beyond that point.

The graph of the temperature at the bottom of the PCM is equal to the one of the top temperature when the PCM is completely solid because the average temperature is calculated. Around t = 1200 the temperature at x=L jumps to the actual temperature so that explains the jump in figure 6.9. The bottom temperature also drops to zero at the end because the code is not defined when all the PCM has melted.

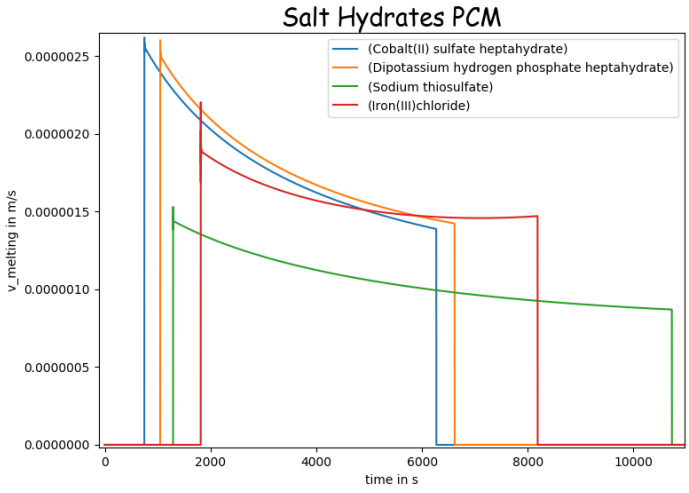

Figure 6.9: The velocity of the melting front of the 4 salt hydrates as PCMs plotted against time.

Figure 6.9 shows the speed of the melting front. This is zero at first and starts when the melting temperature is reached. At this point the graph 'jumps around' a bit. This is due to the structure of the code and should be ignored. When all the PCM has melted the speed drops to zero because there is no more melting front.

Of the salt hydrates Iron(III)chloride, $FeCl_3 \cdot 2\,H_2O$, has the shortest break-even time, this makes sense because it is very cheap. So Iron(III)chloride would make a good PCM material. But because the melting temperature is relatively high other options might be better.

7 Conclusion

This project focused on optimizing the efficiency of a PCM/PV unit. Therefore numerical techniques were developed to generate a model for a PV cell with PCM. The simulations were of a simplified PV cell with already existing PCMs on the economic market. They show that there is quite a difference between the different types of PCMs and their results. The results give a clear indication of which type of PCM has the shortest break-even time. Still, it is important to keep in mind that single PCMs were used and that they were divided into different type of PCMs, like fatty acid and non-paraffins etc. This means that one limitation of our model is that it is not possible to draw a conclusion between the different types of PCMs.

So for example, it cannot be said that paraffins are more suitable as a PCM for a PV cell than fatty acids. The comparison between the best single PCM solely puts the results in perspective, see figure 7.1a, figure 7.1b and figure 7.2. When these PCMs are compared for their break-even point, $FeCl_3 \cdot 2\,H_2O$ of salt hydrates has the shortest break-even time. This PCM has a break-even point of 19 days. The PCM which provides the most extra energy converted is the paraffin C_{26} which converts 66,21 J extra, as seen in table 6.2.

Looking at the comparison between the PCMs you can see that there is a big difference in gradients in the plots among the type of PCMs. This is because of the various values of melting temperature and latent heat. Which of these PCMs is best suitable for a PV cell depends on the aim of the improvement and the local conditions such as air temperature and irradiance. The paraffin C_{26} is capable of having a melting front for the longest period of time. This means that it can absorb heat for the longest time. It also has a very high melting temperature of 56 °C, which make you wonder how effective this will be in a surrounding of 30 °C. On the other hand in the sun objects tend to heat up rapidly to very high temperatures so surrounding temperatures, are less important.

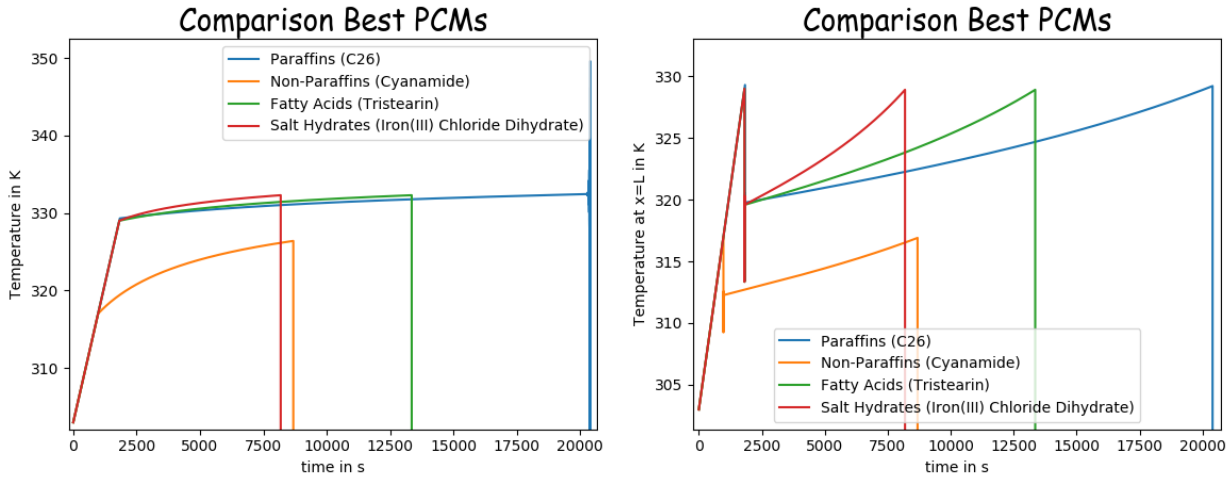

(a) The temperature at the top of the PCM layer

(b) The temperature at the bottom of the PCM layer

Figure 7.1

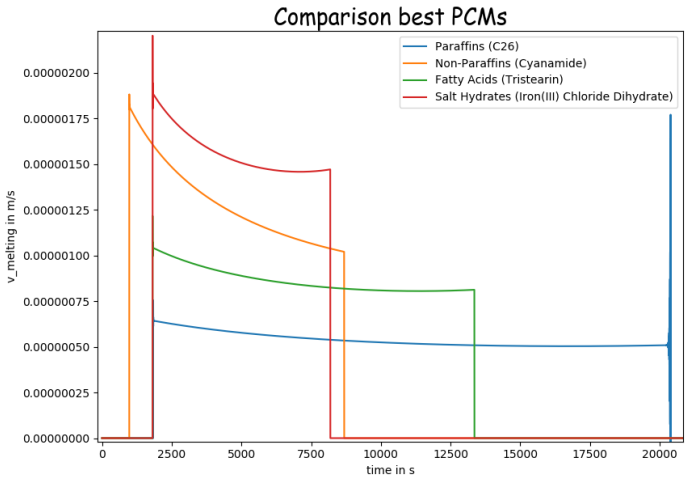

Figure 7.2: The speed of the melting front of the 4 best PCMs plotted against time.

Another important limitation of our model is that all the results of the break-even points of the PCMs are achieved in days. In reality, right now PV cells with PCM take years to come to their break-even point. As we discussed in chapter 5 there are a number of possible explanations. a) The PCM pricing and costs are non realistic. b) The maintenance costs are not included. c) The variability of the weather has not been taken into account. d) The method we used to calculate the average efficiency of the PCM could also be insufficient. We suspect that all these aspects are important, because they influence the performance and estimation of time till break-even point considerably. This would require further research.

For 80% the time in this research project was focused on developing the code. In hind sight we should have spent more time in choosing the main variables for this optimization. However, we reflected on our project process just in time. That's why we were able to discover there were more variables that should have been included into the optimization of the PCM/PV unit, as described above.

As mentioned in chapter 5, there are more limitations to this model because of our simplifications and assumptions. For further research it is suggested to include aspects such as: heat absorption after a liquefied PCM, cooling of PV/PCM during the night and variability of the weather. This could result in a more comprehensive model with more accurate results.

Bibliography

Aroatech. (2021). Paraffin price fluctuation [[Online; accessed 11. Jan. 2021]]. http://iranparaffinwax.com/wiki-paraffin+price+fluctuation-322.html

Baker, E., & Kalowenkamo, J. (2009). Estimating the manufacturing cost of purely organic solar cells. *Solar Energy*, *83*(8), 1224–1231.

Botto, L. (2020). PCM_college1_2020 - WB2543 Process Engineering and Thermodynamics (2020/21 Q2) [[Online; accessed 3. Dec. 2020]]. https://brightspace.tudelft.nl/d2l/le/content/280155/viewContent/2016319/View

Chemicalbook. (2021). PCM prices [[Online; accessed 8. Jan. 2021]]. https://www.chemicalbook.com/Price/ELAIDIC-ACID.htm

Contributors to Wikimedia projects. (2020). *Photovoltaics - Wikipedia* [[Online; accessed 30. Nov. 2020]]. https://en.wikipedia.org/w/index.php?title=Photovoltaics&oldid=991375555

Hasan, A., McCormack, S. J., Huang, M. J., & Norton, B. (2010). Evaluation of phase change materials for thermal regulation enhancement of building integrated photovoltaics. *Sol. Energy*, *84*(9), 1601–1612. https://doi.org/10.1016/j.solener.2010.06.010

Li, Z., Ma, T., Zhao, J., Song, A., & Cheng, Y. (2019). Experimental study and performance analysis on solar photovoltaic panel integrated with phase change material. *Energy*, *178*, 471–486. https://doi.org/10.1016/j.energy.2019.04.166

Ma, T., Yang, H., Zhang, Y., Lu, L., & Wang, X. (2015). Using phase change materials in photovoltaic systems for thermal regulation and electrical efficiency improvement: A review and outlook. *Renewable Sustainable Energy Rev.*, *43*, 1273–1284. https://doi.org/10.1016/j.rser.2014.12.003

Mills A F, C. C. F. M. (2015). *Basic heat and mass transfer*. Temporal publishing.

Nomura, T., Okinaka, N., & Akiyama, T. (2009). Impregnation of porous material with phase change material for thermal energy storage. *Mater. Chem. Phys.*, *115*(2), 846–850. https://doi.org/10.1016/j.matchemphys.2009.02.045

Smith, C. J., Forster, P. M., & Crook, R. (2014). Global analysis of photovoltaic energy output enhanced by phase change material cooling. *Elsevier*. http://eprints.whiterose.ac.uk/81538

Solargis. (2020). Global Solar Atlas [[Online; accessed 13. Jan. 2021]]. https://globalsolaratlas.info/map?c=14.944785,61.875,3&s=18.808524,79.066393%5C%2F&m=site

Stropnik, R., & Stritih, U. (2016). Increasing the efficiency of PV panel with the use of PCM. *Renewable Energy*, *97*, 671–679. https://doi.org/10.1016/j.renene.2016.06.011

Theodore L., e. a. (2011). *Introduction to heat transfer*. John Wiley; Sons.

Wang, R. Z., Xu, Z. Y., & Ge, T. S. (2016). Introduction to solar heating and cooling systems. *Advances in Solar Heating and Cooling* (pp. 3–12). Woodhead Publishing. https://doi.org/10.1016/B978-0-08-100301-5.00001-1

Wenham, S. R. (2011). *Applied photovoltaics*. Routledge.

Wu, X., Lan, S., Zhang, G., Chen, H., & Guo, T. (2019). The effect of light environment during the film formation process on the morphology and function of organic photovoltaics. *J. Mater. Chem. C*, *7*(34), 10584. https://doi.org/10.1039/C9TC03443A